
Bayesian-Optimized Neural Networks with High-Fidelity FEM for Intelligent Residual Strength Prediction in Damaged Ships

[Jianxiao Deng](#), Fei Peng, [Jinlei Mu](#)^{*}, Hailiang Hou

Posted Date: 9 April 2026

doi: 10.20944/preprints202604.0671.v1

Keywords: damaged hull structure; residual ultimate strength; surrogate model; Bayesian regularization; backpropagation neural network (BPNN); nonlinear finite element analysis (NLFEA); parameter optimization; structural reliability



Preprints.org is a free multidisciplinary platform providing preprint service that is dedicated to making early versions of research outputs permanently available and citable. Preprints posted at Preprints.org appear in Web of Science, Crossref, Google Scholar, Scilit, Europe PMC.

Copyright: This open access article is published under a [Creative Commons CC BY 4.0 license](#), which permit the free download, distribution, and reuse, provided that the author and preprint are cited in any reuse.

Disclaimer/Publisher's Note: The statements, opinions, and data contained in all publications are solely those of the individual author(s) and contributor(s) and not of MDPI and/or the editor(s). MDPI and/or the editor(s) disclaim responsibility for any injury to people or property resulting from any ideas, methods, instructions, or products referred to in the content.

Article

Bayesian-Optimized Neural Networks with High-Fidelity FEM for Intelligent Residual Strength Prediction in Damaged Ships

Jianxiao Deng, Fei Peng, Jinlei Mu * and Hailiang Hou

Naval University of Engineering, Wuhan 430033, China

* Correspondence: d22382404@nue.edu.cn; Tel.: 18627122317

Abstract

The rapid and accurate assessment of residual ultimate strength after ship damage is crucial for rescue decision-making and navigation safety, while traditional methods struggle to meet the demands of complex random damage scenarios in terms of efficiency or accuracy. This study proposes a hybrid framework that integrates high-fidelity nonlinear finite element simulation (FEM) and a Bayesian-regularized backpropagation neural network (BPNN). FEM is used to accurately simulate a large number of random damage scenarios, generating a physically credible benchmark dataset. BPNN serves as an efficient surrogate prediction model, with its key parameters—the number of hidden layers and the training algorithm—systematically optimized to enhance generalization capability. The results show that: 1) The FEM simulation results deviate by less than 5% compared to the Smith method, validating the reliability of the dataset. 2) The prediction performance of BPNN is highly dependent on the number of hidden layers and the training algorithm, exhibiting non-monotonic variation, with an optimal parameter combination identified as 8 hidden layers paired with the Bayesian algorithm, achieving a prediction regression value R of 0.91662. 3) Deep networks are prone to overfitting, while shallow networks suffer from insufficient feature capture. 4) The Bayesian algorithm performs best in terms of overfitting resistance and stability. This study not only provides a high-precision and efficient intelligent solution for residual strength assessment of damaged hulls, but its systematic neural network parameter optimization strategy, particularly the approach of identifying optimal depth and selecting anti-overfitting algorithms, also offers important reference for the design of intelligent damage assessment models for similar engineering structures.

Keywords: damaged hull structure; residual ultimate strength; surrogate model; Bayesian regularization; backpropagation neural network (BPNN); nonlinear finite element analysis (NLFEA); parameter optimization; structural reliability

1. Introduction

Structural damage to ships resulting from accidents such as collisions, grounding, or reef strikes can severely compromise their global strength [1]. During subsequent rescue or towing operations, insufficient residual hull strength may lead to further structural failure, potentially causing catastrophic vessel loss or marine environmental pollution [2]. Therefore, the rapid and accurate assessment of the residual ultimate strength of a damaged ship is crucial for ensuring the safety of personnel and assets, as well as for facilitating effective salvage decision-making [3].

The ultimate strength of a ship hull is typically defined as its maximum load-bearing capacity against collapse under global bending moments, commonly characterized by the ultimate bending moment [4]. As external loads increase, the hull structure progressively undergoes yielding, local buckling, and failure until overall collapse occurs. Accurately evaluating this ultimate value,

especially the residual ultimate strength after damage, is essential for determining whether a ship can safely navigate or withstand towing loads in a damaged condition [5].

The assessment of ship hull ultimate strength has long been a core research topic in naval architecture and ocean engineering. The International Association of Classification Societies' Common Structural Rules (CSR) and major classification society regulations include detailed guidelines for ultimate strength assessment [6]. Currently, the main calculation methods include the Smith method, based on the idealized progressive collapse process of structural elements, and high-fidelity nonlinear finite element methods (NFEM). The Smith method is widely adopted in regulations and preliminary design due to its conceptual clarity and relatively high computational efficiency [7]. However, for complex and variable random damage scenarios—such as the high uncertainty in the location, size, and combination of breaches in battle damage—the Smith method has limitations in accurately simulating complex damage modes and their interactions [8]. On the other hand, while NFEM can simulate material nonlinearity, geometric large deformations, and complex damage details with high precision, its computational cost is extremely high, making it difficult to meet the urgent need for rapid assessment of numerous potential damage scenarios in battle damage or emergency response situations [9].

This trade-off between efficiency and accuracy significantly hinders the application of residual strength assessment in real-time decision-making support for damaged ships [10]. In recent years, machine learning methods, particularly artificial neural networks, have shown great potential in structural response prediction due to their powerful nonlinear mapping capabilities and efficient inference characteristics [11]. For instance, in ship stability prediction, machine learning models integrating multiple regression trees can effectively predict the probability of ship instability [12]. In the prediction of fatigue life for defective materials, physics-informed neural networks (PINNs) combined with linear elastic fracture mechanics (LEFM) can more accurately predict the finite fatigue life of materials by integrating experimental data and physical constraints [13]. Furthermore, neural networks have been applied to assess the ultimate strength of hull grillages under multiple crack damages, investigating the influence of factors such as crack angle, length, and location through the combination of nonlinear finite element methods (FEM) and artificial neural networks (ANN) [14]. In damage identification, a novel method combining the boundary element method (BEM) and cascade neural networks can predict the presence, location, classification, and extent of damage in plates with high precision and efficiency [15]. Among these, backpropagation (BP) neural networks have been attempted for predicting the ultimate strength of hull girders [14]. However, existing studies often lack systematic optimization of key neural network parameters—such as network depth and training algorithms—leading to insufficient generalization capability, and unreliable prediction accuracy and robustness [16]. This is particularly true when processing datasets generated from high-fidelity simulations that reflect complex physical mechanisms, where inadequately optimized neural network models are prone to underfitting or overfitting.

To address these challenges, this paper proposes and investigates a hybrid intelligent prediction framework that integrates high-fidelity nonlinear finite element simulation (NFEM) and a Bayesian-regularized backpropagation neural network (BPNN). The core research objective is to achieve efficient and high-precision prediction of the residual load-bearing capacity of damaged hulls. The technical roadmap of this study is illustrated in Figure 1. First, a validated NFEM is used to simulate and generate a large, high-reliability dataset covering random damage scenarios. Second, a BPNN prediction model is constructed, and the influence of key parameters—such as the number of hidden layers and training algorithms—on its prediction performance (accuracy, generalization, efficiency) is systematically studied to identify the optimal configuration. Finally, a data-driven, efficient assessment solution for engineering practice is developed. This study not only provides a new method for damaged hull safety assessment but also offers a systematic neural network parameter optimization strategy as an important reference for designing intelligent damage assessment models for similar engineering structures.

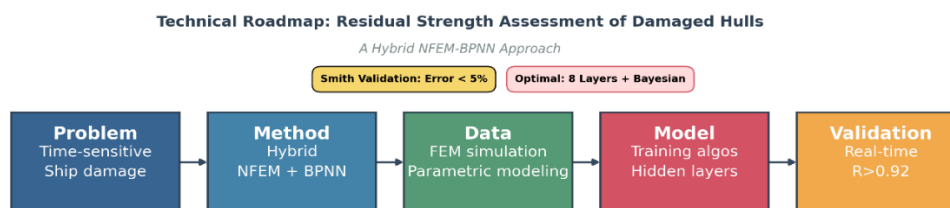


Figure 1. Technical Roadmap.

2. Research on Calculation Methods for Ultimate Strength of Damaged Ship Hulls

The ultimate strength of a ship hull refers to its maximum load-bearing capacity against collapse under global bending moments, typically characterized by the ultimate bending moment. Accurately assessing the residual ultimate strength of a damaged hull is crucial for ensuring the navigation safety of the impaired vessel and formulating rescue and towing plans. Currently, the main calculation methods for ship hull ultimate strength include direct calculation methods (analytical methods), simplified progressive collapse methods (Smith method), idealized structural unit methods (ISUM), and nonlinear finite element methods (NFEM). This section reviews and analyzes the core principles, characteristics, and applicability of these methods.

2.1. Direct Calculation Method

Direct calculation methods primarily rely on empirical formulas and theoretical derivations for rapid estimation of ship hull ultimate strength [17]. Their significant advantage lies in high computational efficiency and minimal required input parameters, making them suitable for preliminary engineering design and rapid assessment scenarios.

However, this method has inherent limitations: its simplified models struggle to accurately simulate the complex progressive collapse process of hull structures under global bending moments (such as material yielding, local buckling, and their interactions), failing to reflect the true mechanisms of structural failure. Therefore, results from analytical methods are generally used as preliminary references, with accuracy often insufficient for high-fidelity assessment needs, particularly when dealing with complex damage scenarios.

2.2. Simplified Progressive Collapse Method (Smith Method)

The simplified progressive collapse method, proposed by Smith in 1977, is based on the concept that hull girder collapse is a process of sequential component failure [18]. This method discretizes the hull cross-section into several basic units (such as hard-corner units, stiffened panel units, and plate units) [19]. Under incrementally applied curvature loads, the following steps are performed:

1. Calculate the strain of each unit based on the assumption of a plane cross-section and the instantaneous position of the neutral axis.
2. Determine the stress using each unit's average stress-strain relationship (considering failure modes such as tensile yielding and compressive buckling).
3. Calculate the total axial force of the cross-section and iteratively adjust the neutral axis position until the total axial force is zero.
4. Calculate the bending moment of the cross-section for the current curvature by summing the moments of each unit's stress about the instantaneous neutral axis.
5. Plot the moment-curvature curve; the peak moment corresponds to the ultimate moment.

For damaged hulls, the Smith method effectively handles asymmetric cross-sections and hull inclination caused by compartment flooding by dynamically adjusting the instantaneous neutral axis

(translation and rotation) to reflect the mechanical behavior of the remaining effective cross-section [20].

The advantages of the Smith method include: clear physical significance and a good representation of the progressive collapse process of the hull. Its computational efficiency is significantly higher than that of high-fidelity simulations, making it one of the standard methods adopted by the International Association of Classification Societies (IACS) Common Structural Rules for tankers and bulk carriers (CSR/H-CSR) and major classification society regulations for ultimate strength assessment [21].

Its limitations include: reliance on idealized unit stress-strain relationships, which may introduce errors; challenges in accurately simulating highly complex or random damage modes (such as multiple irregular breach locations and their interactions in battle damage) and complex material nonlinearity and large deformation effects; and dependence on whether the model satisfies basic assumptions (such as the plane cross-section assumption).

2.3. Idealized Structural Unit Method (ISUM)

The Idealized Structural Unit Method (ISUM) is a semi-analytical approach situated between analytical methods and finite element methods [22]. Its core concept involves dividing complex structures into a series of idealized units (such as stiffened panel units) with predefined simplified failure behavior modes under load (such as column buckling, torsional buckling, and web local buckling).

The main advantage of ISUM is that, with reasonable unit partitioning, its computational accuracy can approach that of nonlinear finite element methods while maintaining much higher computational efficiency.

However, a key challenge of ISUM lies in the significant impact of unit idealization on computational accuracy. For actual complex hull structures, particularly those with damage, accurately and reasonably selecting and defining these idealized units is difficult [23]. This high dependence on modeling expertise limits the widespread application of ISUM in engineering practice.

2.4. Nonlinear Finite Element Method (NFEM)

The Nonlinear Finite Element Method (NFEM) is based on variational principles, discretizing the hull structure into a finite number of elements and solving highly nonlinear governing equations through numerical iteration. It can simulate the entire process of hull collapse from initial loading to overall failure with high precision [24]. Therefore, NFEM is widely recognized as the most accurate method for calculating ship hull ultimate strength, especially the residual strength in the presence of complex damage [25].

The main disadvantage of NFEM is its extremely high computational cost. Simulating a hull compartment model with complex nonlinear behavior and damage until collapse typically requires several hours or even days of computation. This high computational expense makes it difficult to directly apply NFEM to scenarios requiring rapid assessment of numerous random damage scenarios, such as battle damage assessment or emergency response.

In summary, the four main methods for calculating ship hull ultimate strength each have their applicable scope, advantages, and disadvantages, as summarized in Table 1.

Table 1. Comparison of Hull Ultimate Strength Calculation Methods.

Method	Core Principle	Main Advantages	Main Limitations	Applicable Scenarios
Direct Calc.	Empirical formulas & theoretical derivation	Very fast, few input parameters	Limited accuracy, cannot simulate failure process	Preliminary design, rapid rough assess.
Smith Method	Section discretization, unit progressive fail	Clear concept, efficient, code-accepted	Limited simulation of complex damage & nonlinearity, relies on unit constitutive	Code compliance, standard damage assess
ISUM	Idealized units & simplified failure modes	Accuracy close to NFEM, relatively efficient	Unit discretization highly experience-dependent, complex modeling	Specific structures studies, efficiency and accuracy trade-off
NFEM	FE discretization, solve nonlinear eqns.	Highest accuracy, simulates full process & complex effects	Extremely high computational cost	High-precision research, complex damage assessment

The research objective of this paper is to construct a high-precision, physically credible dataset of residual strength for damaged hulls to train neural network models, requiring extremely high accuracy and reliability of the data itself. While the Smith method is relatively efficient and widely recognized, it is insufficient for accurately simulating random, complex damage modes and the resulting strongly nonlinear behavior. Although NFEM faces computational efficiency challenges, its capabilities in simulation accuracy and capturing complex physical mechanisms are irreplaceable [26]. Therefore, this paper selects the Nonlinear Finite Element Method (NFEM) as the core tool for generating the benchmark dataset.

To verify the reliability of NFEM simulation results, Section 4 of this paper will systematically compare NFEM calculation results with those of the widely used Smith method. After confirming that NFEM accuracy meets requirements, it will be used to efficiently generate a large amount of high-quality data covering different random damage scenarios, laying a solid foundation for the subsequent intelligent prediction model based on the BP neural network. Section 3 will elaborate in detail on the modeling and simulation process of damaged hull structures based on NFEM.

3. Modeling and Simulation of Damaged Hull Structures

When calculating the ultimate strength of a ship hull girder using nonlinear finite element analysis, both the software's computational capabilities and time costs must be considered. To compute the ultimate load-bearing capacity, a specific compartment model with appropriate boundary conditions must be selected to satisfy the calculation requirements. Common compartment length selection methods include four patterns, as shown in Table 2:

Table 2. Common Hull Segment Selection Methods.

Segment Mode	Selection Method
Two Trans. Frames	Select the segment length between two transverse frames for modeling
Two Trans. Bulkheads	Select the segment length between two transverse bulkheads for modeling
1/2+1+1/2	Select one full central segment, extending half a segment length forward and aft

1+1+1	Select one full central segment, extending one full segment length forward and aft
-------	--

Among these four selection methods, the first is insufficient for considering the overall instability of the full compartment deck. Among the remaining three, the latter two methods, with extended sections on both ends, can eliminate boundary condition effects. In ship finite element modeling, the transverse range covers the full ship width, and the vertical range covers the entire molded depth. This paper adopts the 1/2+1+1/2 compartment pattern and establishes a hull structure compartment model, as shown in Figure 2:

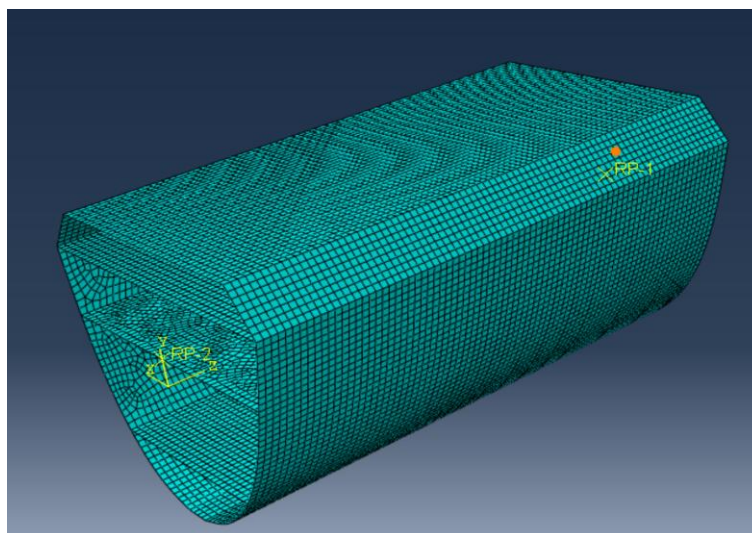


Figure 2. Hull Structural Segment Model.

The model employs three-dimensional shell elements, primarily using reduced-integration quadrilateral elements (S4R). Material properties are defined as follows: Poisson's ratio $\nu = 0.3$, Young's modulus $E = 2.06 \times 10^5$ MPa, steel density $\rho = 7.85 \times 10^{-9}$ t/mm³. Material plasticity is defined according to Table 3:

Table 3. Material Plasticity Parameters.

Yield Stress (MPa)	Plastic Strain
235.0	0
248.0	0.00124
294.5	0.03936
332.5	0.07749
362.0	0.11562
383.0	0.15370
395.7	0.19187
399.9	0.23000

The positive x-axis direction is along the ship length toward the bow; the z-axis is vertical with upward as positive; the positive y-axis direction is along the ship width toward the starboard side. ABAQUS has multi-point constraint (MPC) functionality, allowing the creation of a rigid region by connecting all nodes on the planes at both ends of the compartment model to reference points. To simulate the hull failure process under vertical loads, two reference points, RP-1 and RP-2, are created at the centroids of the planes at the model's forward and aft ends, respectively. These reference points are rigidly connected to all nodes within their respective end planes. Due to the rigid connection, the boundary conditions of the model end planes will be consistent with those of the reference points.

After establishing the hull structure compartment model, ABAQUS Boolean operations are used to subtract the breach model from the compartment model, simulating various damage scenarios.

This section selects damage scenarios with breach sizes of 2, 3, 4, and 5 meters, located at the mid-length and mid-depth of the compartment. Reference point RP-2 is fully fixed, while a rotation about the x-axis is applied to reference point RP-1. The applied rotation angle can be estimated based on the initial buckling moment. Finally, the output sectional reaction moment is analyzed to plot the moment-rotation curve. The peak value of this curve corresponds to the ultimate bending moment of the ship.

4. Error Comparison Between Smith Method and Nonlinear FEM

The specific steps for calculating the ultimate bending moment using the simplified progressive collapse method are as follows:

1. Selection of Cross-Section: Choose a typical cross-section from the hazardous area of the hull. The distribution of longitudinal bending moments along the ship length typically peaks at the midship section and decreases toward the bow and stern. For intact ships, the hazardous section is generally selected from the midship compartment. For battle-damaged ships, the section with the breach is typically selected.
2. Discretization of Structural Units: Discretize the longitudinal structural members of the selected cross-section into hard-corner units, stiffened panel units, and plate units.

Hard-corner units: Mainly refer to plates at intersections or corner regions, assumed not to buckle within the yield limit and failing in an elastic-perfectly plastic mode.

Stiffened panel units: Consist of stiffeners and their associated plating. Under tension, they fail in an elastic-perfectly plastic mode; under compression, they exhibit failure modes such as column buckling, torsional buckling, and web local buckling.

Plate units: Plates between stiffeners, between a stiffener and a hard-corner unit, or larger plates between two hard-corner units.

3. Determination of Stress-Strain Relationships: Define the stress-strain relationships for the discretized units.
4. Calculation of Maximum Curvature in Incremental Iteration: Apply a small curvature increment in each step. Calculate the neutral axis position for the initial curvature increment.
5. Strain and Stress Calculation: Calculate the strain of each unit under the current curvature. Determine the corresponding stress and axial force of each unit using its stress-strain relationship.
6. Neutral Axis Adjustment: Sum the axial forces of all units in the cross-section to obtain the total axial force. Adjust the neutral axis position iteratively until the total axial force is zero, determining the true neutral axis position for that curvature.
7. Bending Moment Calculation: Sum the contributions of each unit's axial force to the sectional bending moment about the neutral axis, obtaining the moment for the initial curvature increment.
8. Iterative Process: Increase the curvature, using the current neutral axis height as the initial value for the next curvature step. Repeat steps 5-7 iteratively to obtain the sectional moment for each curvature. Finally, plot the moment-curvature curve for the cross-section. The moment corresponding to zero slope of this curve is the ultimate bending moment.

Under battle damage conditions, accurately calculating the environmental loads and compartment flooding states the ship experiences can be difficult and time-consuming for rapid assessment. Therefore, the residual load-bearing capacity at the damaged section can be assessed using the ratio C_R of the ultimate bending moment in the damaged condition M_{UD} to that in the intact condition M_U :

$$C_R = \frac{M_{UD}}{M_U} \times 100\% \quad (1)$$

This paper applies the Smith method to calculate the residual load-bearing capacity for the same damage scenarios as those in Section 3 (nonlinear finite element method) and compares the results with the finite element method, as shown in Table 4:

Table 4. Error Comparison of Results between Smith Method and FEM.

Moment Breach Size (m)	Damaged Ult. Moment (10 ⁹ N·m)			Intact Ult. Moment (10 ⁹ N·m)			Residual Capacity (%)		
	Smith	NFEM	Error	Smith	NFEM	Error	Smith	NFEM	Error
1	1.64	1.60	2.44%				99.39%	99.38%	0.02%
1.5	1.62	1.58	2.47%				98.18%	98.14%	0.05%
2	1.60	1.56	2.50%				96.97%	96.89%	0.08%
2.5	1.57	1.53	2.55%				96.15%	95.03%	0.13%
3	1.53	1.49	2.61%	1.65	1.61	2.42%	92.73%	92.55%	0.19%
3.5	1.50	1.46	2.67%				90.91%	90.68%	0.25%
4	1.47	1.43	2.72%				89.09%	88.82%	0.30%
4.5	1.44	1.40	2.78%				87.27%	86.96%	0.36%
5	1.42	1.38	2.82%				86.06%	85.71%	0.40%

As a relatively mainstream method for calculating ultimate strength, the Smith method yields reasonably accurate results. Analysis of the nonlinear finite element method results shows that the calculated damaged ultimate bending moment and intact bending moment data differ from the Smith method results by no more than 5%. Moreover, the final calculated residual load-bearing capacities are very similar. The comparison results indicate that the nonlinear finite element method provides reliable accuracy for assessing the residual load-bearing capacity of damaged hulls, meeting the requirements for generating a high-quality dataset. This method can thus be used to simulate numerous scenarios, enriching the dataset for neural network learning and training, thereby enhancing the stability and reliability of the constructed prediction model.

5. Training and Parameter Optimization of the BP Neural Network

5.1. Data Preprocessing

The structural composition of a BP neural network is illustrated in Figure 3. Its training process generally consists of two main parts: forward propagation of working signals and backward propagation of error signals. 1) Feature parameters enter the neural network, are processed by the hidden layers, and reach the output layer, where they are transformed into output signals and compared with the expected output values. 2) The difference between the output signals and the expected outputs constitutes the error, which is converted into an error signal and propagated backward from the output layer. This training process is repeated until the neural network's training accuracy requirements are met, ultimately aligning the network's output signals with the expected values.

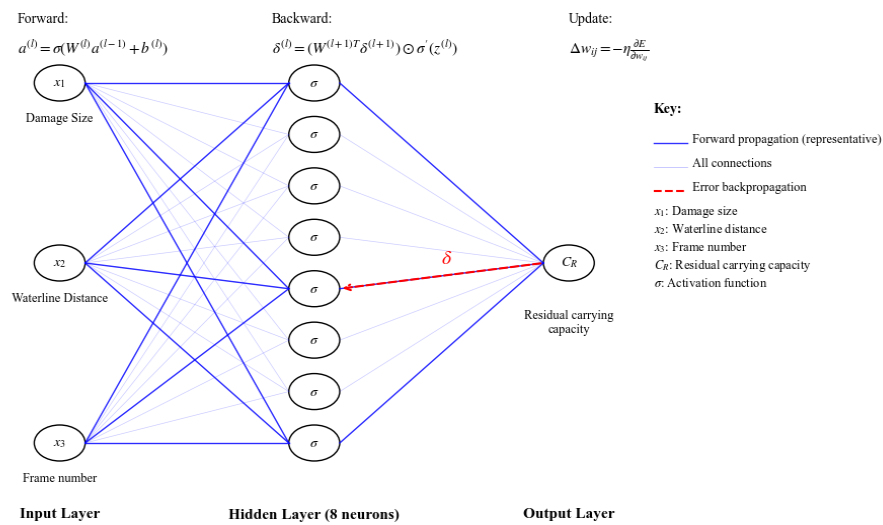


Figure 3. BP Neural Network Structure.

To comprehensively and effectively reflect breach information, this paper employs the Min-Max normalization method to scale breach location and size data to the range [0, 1]. The basic formula for Min-Max normalization is:

$$X' = \frac{x - \min(x)}{\max(x) - \min(x)} \quad (2)$$

where X' is the normalized data, obtained by dividing the difference between the sample data and the sample minimum by the range (sample maximum minus sample minimum). Thus, X' is a value within 0–1. Given X' , denormalization can revert the data to its actual range. Processed data not only unify dimensions but also lead to higher training accuracy and better recognition performance when used as feature parameters in neural networks.

5.2. BP Neural Network Training

This paper normalizes the data obtained from the Smith method and nonlinear finite element method to form a dataset. The breach frame number, distance of the breach from the waterline, and breach size are used as input data, while the residual load-bearing capacity serves as the target data for neural network learning and training. Specifically, 60% of the data is used as the training set, with 20% each allocated to the validation and test sets.

The number of hidden layers in the neural network is set to 10, and training begins using the Levenberg-Marquardt algorithm. As shown in Figure 4, the error histogram visually displays the errors between predicted outputs and target outputs. The horizontal axis represents the magnitude of the error (positive or negative), while the vertical axis indicates the count of samples with corresponding error magnitudes. Blue bars represent training data, green bars represent validation data, and red bars represent test data. It can be observed that the majority of data errors are within 0.1, with most errors within 0.03, indicating relatively small errors.

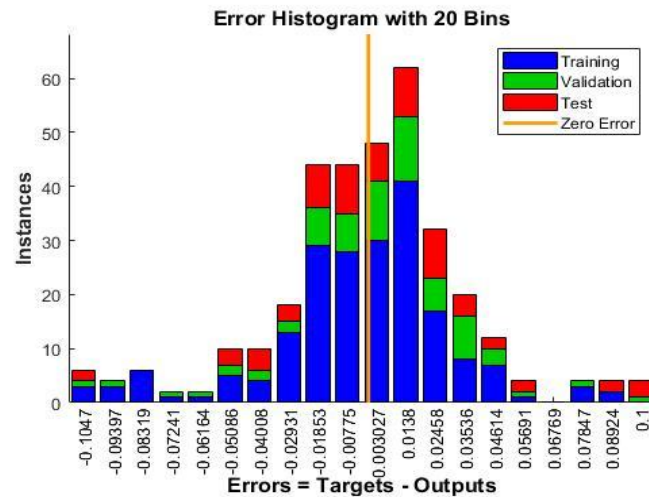


Figure 4. Error Histogram.

As shown in Figure 5, the regression plot displays the network outputs against the targets for the training, validation, and test sets. The regression value R represents the correlation between predicted outputs and target outputs. An R value closer to 1 indicates a stronger relationship between predicted and output data, while an R value closer to 0 suggests greater randomness in the relationship. For a perfect fit, data points should fall along a 45-degree line where network outputs equal targets. The plot includes data correlation relationships for the training, validation, test, and overall sets after training. The horizontal axis represents target outputs, and the vertical axis represents the fitted function between predicted outputs and target outputs. The results show an overall regression R value above 0.85, indicating good performance.

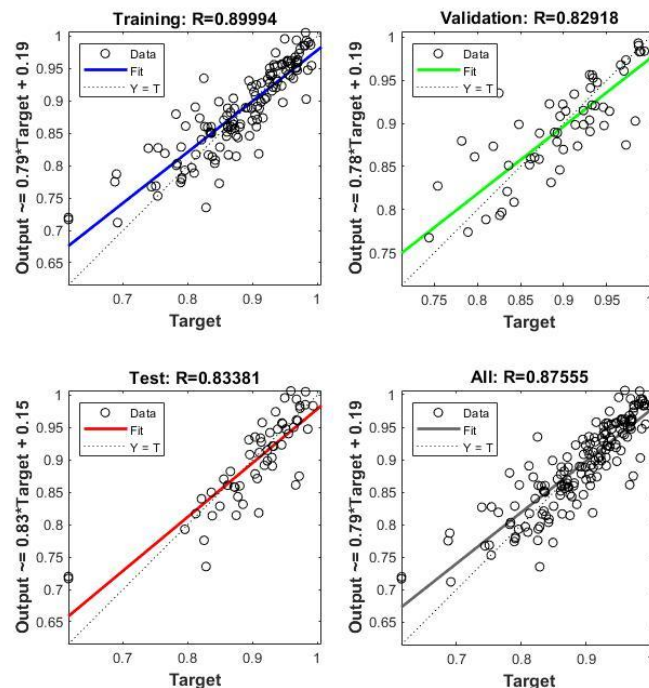


Figure 5. Linear Regression Plot.

As shown in Figure 6, the mean squared error (MSE) represents the average squared difference between predicted outputs and target outputs. Lower values are better, with 0 indicating no error. The horizontal axis represents the number of training iterations, and the vertical axis denotes the MSE value. The green circle in the plot indicates the iteration number and MSE value when the validation set achieves the best MSE, which is 0.0012908 at 11 iterations.

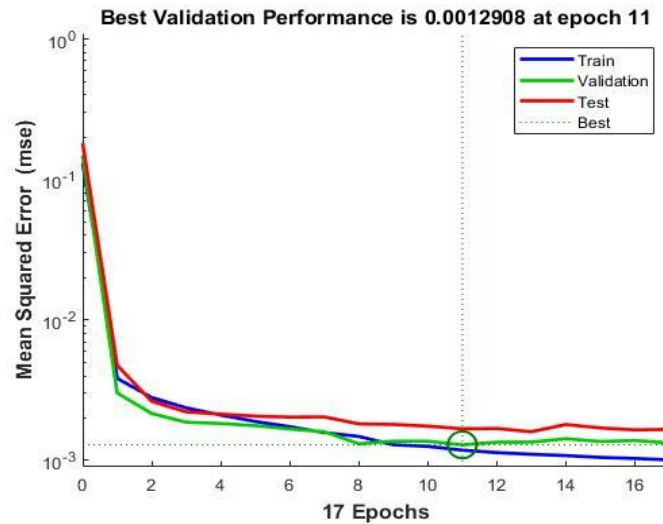


Figure 6. Mean Squared Error Iteration Curve.

5.3. Optimization Study of Training Parameters

uring neural network training, different algorithms—including Levenberg-Marquardt (L-M), Bayesian regularization (Bayesian), and Scaled conjugate gradient (Scaled)—can be selected, and the number of hidden layers in the neural network can be varied. This paper selects different algorithms and varying numbers of hidden layers to train the neural network, resulting in 15 configurations combining five hidden layer counts and three training algorithms. Each configuration undergoes five training runs to eliminate the influence of random initialization, with the average performance reported. As shown in Table 5, the regression value R is selected as the evaluation metric for neural network training effectiveness, and the training outcomes are compared.

Table 5. Neural Network Training Performance Comparison.

Hidden Layers	Training Algorithm	Regression Value (R)
2	Levenberg-Marquardt (L-M)	0.74981
	Bayesian Regularization (Bayesian)	0.78859
	Scaled Conjugate Gradient(Scaled)	0.40905
4	Levenberg-Marquardt (L-M)	0.75006
	Bayesian Regularization(Bayesian)	0.77151
	Scaled Conjugate Gradient(Scaled)	0.74372
6	Levenberg-Marquardt (L-M)	0.87798
	Bayesian Regularization(Bayesian)	0.89509
	Scaled Conjugate Gradient(Scaled)	0.77623
8	Levenberg-Marquardt (L-M)	0.85691
	Bayesian Regularization(Bayesian)	0.91662
	Scaled Conjugate Gradient(Scaled)	0.76335
10	Levenberg-Marquardt (L-M)	0.87555
	Bayesian Regularization(Bayesian)	0.92622
	Scaled Conjugate Gradient(Scaled)	0.74106

As shown in Figure 7, neural network training effectiveness exhibits significant dependence on both the method and structure:

1. Training Function Sensitivity Analysis: The Scaled algorithm performs weakest in shallow networks (e.g., 2 hidden layers), with $R=0.40905$, indicating insufficient capability to capture features of ship damage data. In contrast, the Bayesian algorithm demonstrates the best fitting performance, followed by the L-M algorithm.
2. Nonlinear Effect of Hidden Layer Depth: When the number of hidden layers increases to 6, the L-M and Scaled algorithms reach peak performance, with regression R values of 0.87798 and 0.77623, respectively. Further increasing the layer count leads to a decline in training effectiveness. The Bayesian algorithm's performance saturates at 8 hidden layers, with $R=0.91662$ for 8 layers and $R=0.92622$ for 10 layers, showing less than a 1% improvement. This indicates that model complexity must match problem complexity, and blindly increasing the number of hidden layers may lead to overfitting.
3. Overfitting Phenomenon Diagnosis: Overfitting occurs when there is a large gap between training error and test error. In other words, the model complexity exceeds the actual problem complexity, leading to excellent performance on the training set but poor performance on the test set. The model essentially "memorizes" the training set without understanding the underlying data patterns, resulting in poor generalization. In deep networks (more than 6 hidden layers), a phenomenon occurs where training set error continues to decrease, while validation and test set errors increase significantly. This aligns with typical overfitting characteristics, as seen with the Scaled function in Figure 7, where validation error spikes at 10 layers, degrading generalization. The underlying cause is that model capacity exceeds the complexity of the true data distribution. This phenomenon can be automatically constrained by Bayesian optimization of network depth.

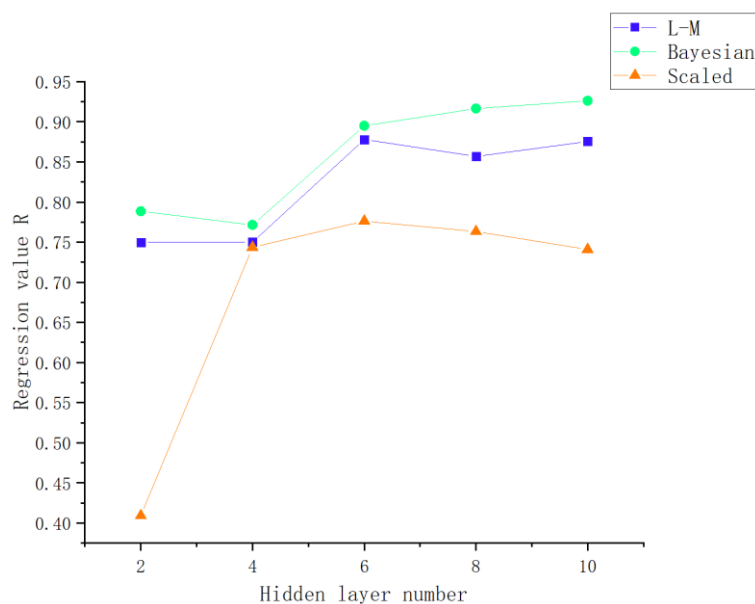


Figure 7. Neural Network Training Performance Evaluation.

For the problem of residual load-bearing capacity prediction of damaged hulls, the following parameter optimization scheme is proposed:

1. Algorithm Priority: Bayesian > L-M >> Scaled

Bayesian algorithm: Strong resistance to overfitting, best stability in deep networks, $R > 0.91$ for 8–10 layers.

L-M algorithm: Suitable for medium-depth networks, peaks at 6 layers with $R=0.878$, fast convergence.

Scaled algorithm: Only viable at 6 layers, $R=0.776$, significantly degraded performance at other depths.

2. Layer Optimization Principles:

Lightweight Architecture: Prioritize 8 layers + Bayesian, $R=0.91662$, balancing accuracy and efficiency.

Avoid Excessive Depth: For layers > 8 , Bayesian shows marginal improvement ($<1\%$) but drastically increases computational resource consumption and may induce overfitting.

Avoid Shallow Networks: For layers < 6 , all algorithms yield $R<0.79$, indicating insufficient feature capture.

In summary, for the data type in this study, the optimal neural network parameter choice is 8 hidden layers + Bayesian training function, with a regression R of 0.91662. This configuration offers the highest accuracy, minimal overfitting risk, and reasonable resource consumption. The suboptimal choice is 6 hidden layers + L-M training function, with $R=0.87798$, suitable for scenarios requiring high-speed training. Configurations to avoid include: layers ≤ 4 (insufficient accuracy) or the Scaled algorithm (unstable). Additionally, for layers > 8 , accuracy improvement is less than 1% and carries overfitting risks.

6. Conclusions

To address the need for rapid and precise assessment of residual bearing capacity following ship battle damage, this study proposed and validated a hybrid intelligent prediction framework integrating high-fidelity nonlinear finite element simulation (FEM) and a Bayesian-regularized backpropagation neural network (BPNN). Through systematic research, the following main conclusions were drawn:

1. Reliability Verification of High-Fidelity FEM Dataset: Using Abaqus software, hull structural responses under various damage scenarios (different breach sizes and locations) were accurately simulated, successfully calculating ultimate bending moments and residual load-bearing capacities. Comparative validation with the widely recognized Smith method confirmed that discrepancies between the two methods for damaged ultimate bending moments, intact ultimate bending moments, and residual load-bearing capacity ratios were all less than 5%. This fully demonstrates the high reliability of the FEM simulation results, laying a solid foundation for constructing a high-quality, physically credible benchmark dataset that meets the requirements for data accuracy and diversity in subsequent neural network training.
2. Successful Construction and Core Value of BPNN Prediction Model: A BPNN model was successfully trained using the high-quality dataset generated by FEM, achieving efficient prediction of residual load-bearing capacity for damaged hulls. The core advantage of this model lies in its significant improvement in computational efficiency, enabling near real-time predictions. This overcomes the bottleneck of traditional FEM's lengthy computation times for complex random damage scenarios, providing a powerful tool for rapid wartime assessment and decision-making.
3. Systematic Findings and Key Strategies for Neural Network Parameter Optimization: This study deeply revealed the high dependence and non-monotonic variation of BPNN prediction performance on network structure (number of hidden layers) and training algorithm, successfully identifying the optimal parameter combination:

Effect of Hidden Layer Depth: Prediction accuracy does not increase monotonically with the number of hidden layers; an optimal range exists (6–8 layers). Networks that are too shallow (<6 layers) suffer from insufficient feature capture ($R<0.79$), leading to underfitting, while networks that are too deep (>8 layers) are prone to overfitting, degrading generalization.

Training Algorithm Preference: The Bayesian regularization algorithm performs best in terms of overfitting resistance and model stability, particularly excelling in deep networks. The L-M algorithm

offers fast convergence and suboptimal performance in medium-depth networks (6 layers). The Scaled algorithm generally performs weaker and is less stable.

Confirmation of Optimal Combination: For the dataset in this study, 8 hidden layers paired with the Bayesian regularization training algorithm is identified as the optimal parameter combination, achieving a high prediction regression value RR of 0.92622, striking the best balance between prediction accuracy, generalization capability, and computational resource consumption. Six hidden layers paired with the L-M algorithm ($R=0.87798$) serves as a suboptimal choice balancing speed and accuracy.

The hybrid framework of “FEM-generated data + BPNN intelligent prediction + systematic parameter optimization” proposed in this study successfully achieves high-precision and efficient assessment of residual load-bearing capacity for damaged hulls. More importantly, the systematic neural network parameter optimization strategy employed—specifically, the identification of optimal network depth and the selection of anti-overfitting algorithms—holds significant methodological value. It provides a reusable reference paradigm for designing intelligent rapid assessment models for complex structures under random damage conditions in naval architecture and other engineering fields.

Author Contributions: Deng Jianxiao: Conceptualization, Methodology, Software, Writing—Original Draft; Peng Fei: Validation, Formal analysis, Data Curation; Mu Jinlei*: Supervision, Project administration, Writing—Review & Editing, Funding acquisition; Hou Hailiang: Resources, Visualization, Investigation.

Conflicts of Interest: The authors declare that they have no known competing financial interests or personal relationships that could have appeared to influence the work reported in this paper.

References

1. Zhang, Y. et al. (2021) “Study on the unequivalence between stiffness loss and strength loss of damaged hull girder,” *Ocean Engineering*, 229, p. 108986. Available at: <https://doi.org/10.1016/j.oceaneng.2021.108986>.
2. Kuznecovs, A. et al. (2020) “Ultimate limit state analysis of a double-hull tanker subjected to biaxial bending in intact and collision-damaged conditions,” *Ocean Engineering*, 209, p.107519. Available at: <https://doi.org/10.1016/j.oceaneng.2020.107519>.
3. Zhu, Z. et al. (2024) “A novel method for determining the neutral axis position of the asymmetric cross section and its application in the simplified progressive collapse method for damaged ships,” *Ocean Engineering*, 301, p. 117390. Available at: <https://doi.org/10.1016/j.oceaneng.2024.117390>.
4. Cerik, B.C. and Choung, J. (2020) “Progressive Collapse Analysis of Intact and Damaged Ships under Unsymmetrical Bending,” *Journal of Marine Science and Engineering*, 8(12), p. 988. Available at: <https://doi.org/10.3390/jmse8120988>.
5. Tabri, K., Naar, H. and Kōrgesaar, M. (2020) “Ultimate strength of ship hull girder with grounding damage,” *Ships and Offshore Structures*, 15(sup1), pp. S161–S175. Available at: <https://doi.org/10.1080/17445302.2020.1827631>.
6. Parunov, J., Mikulić, A. and Čorak, M. (2024) “Consequences of the Improved Wave Statistics on a Hull Girder Reliability of Double Hull Oil Tankers,” *Journal of Marine Science and Engineering*, 12(4), p. 642. Available at: <https://doi.org/10.3390/jmse12040642>.
7. “A study on the progressive collapse behaviour of a damaged hull girder” (2014) in *Maritime Technology and Engineering*. CRC Press, pp. 423–434. Available at: <https://doi.org/10.1201/b17494-46>.
8. Zhu, Z. et al. (2020) “Ultimate Limit State Function and Its Fitting Method of Damaged Ship under Combined Loads,” *Journal of Marine Science and Engineering*, 8(2), p. 117. Available at: <https://doi.org/10.3390/jmse8020117>.
9. Parunov, J., Prebeg, P. and Rudan, S. (2020) “Post-accidental structural reliability of double-hull oil tanker with near realistic collision damage shapes,” *Ships and Offshore Structures*, 15(sup1), pp. S190–S207. Available at: <https://doi.org/10.1080/17445302.2020.1789035>.

10. Zeng, H. et al. (2024) "High-Accuracy and Fast Calculation Framework for Berthing Collision Force of Docks Based on Surrogate Models," *Journal of Marine Science and Engineering*, 12(6), p. 898. Available at: <https://doi.org/10.3390/jmse12060898>.
11. Li, H., Jiao, H. and Yang, Z. (2023) "Ship trajectory prediction based on machine learning and deep learning: A systematic review and methods analysis," *Engineering Applications of Artificial Intelligence*, 126, p. 107062. Available at: <https://doi.org/10.1016/j.engappai.2023.107062>.
12. Jiang, C., Xiang, X. and Xiang, G. (2024) "A joint multi-model machine learning prediction approach based on confidence for ship stability," *Complex & Intelligent Systems*, 10(3), pp. 3873–3890. Available at: <https://doi.org/10.1007/s40747-024-01363-w>.
13. Niu, X. et al. (2024) "Defect sensitivity and fatigue design: Deterministic and probabilistic aspects in additively manufactured metallic materials," *Progress in Materials Science*, 144, p. 101290. Available at: <https://doi.org/10.1016/j.pmatsci.2024.101290>.
14. Li, D. et al. (2022) "Ultimate strength assessment of ship hull plate with multiple cracks under axial compression using artificial neural networks," *Ocean Engineering*, 263, p. 112438. Available at: <https://doi.org/10.1016/j.oceaneng.2022.112438>.
15. Yang, Y., Zhan, Z. and Liu, Y. (2024) "A novel damage identification algorithm by combining the boundary element method and a series connection neural network," *Engineering Applications of Artificial Intelligence*, 133, p. 108010. Available at: <https://doi.org/10.1016/j.engappai.2024.108010>.
16. Kim, Y.-C. et al. (2023) "Power Prediction Method for Ships Using Data Regression Models," *Journal of Marine Science and Engineering*, 11(10), p. 1961. Available at: <https://doi.org/10.3390/jmse11101961>.
17. Crupi, V., Epasto, G. and Guglielmino, E. (2013) "Comparison of aluminium sandwiches for lightweight ship structures: Honeycomb vs. foam," *Marine Structures*, 30, pp. 74–96. Available at: <https://doi.org/10.1016/j.marstruc.2012.11.002>.
18. Kuznecovs, A., Schreuder, M. and Ringsberg, J.W. (2021) "Methodology for the simulation of a ship's damage stability and ultimate strength conditions following a collision," *Marine Structures*, 79, p. 103027. Available at: <https://doi.org/10.1016/j.marstruc.2021.103027>.
19. Cui, H. et al. (2024) "Ultimate strength assessment of hull girders considering elastic shakedown based on Smith's method," *Ocean Engineering*, 293, p. 116695. Available at: <https://doi.org/10.1016/j.oceaneng.2024.116695>.
20. Zhu, Z. et al. (2024) "A novel method for determining the neutral axis position of the asymmetric cross section and its application in the simplified progressive collapse method for damaged ships," *Ocean Engineering*, 301, p. 117390. Available at: <https://doi.org/10.1016/j.oceaneng.2024.117390>.
21. Li, S., Kim, D.K. and Benson, S. (2021) "A probabilistic approach to assess the computational uncertainty of ultimate strength of hull girders," *Reliability Engineering & System Safety*, 213, p. 107688. Available at: <https://doi.org/10.1016/j.res.2021.107688>.
22. Paik, J.K., Seo, J.K. and Kim, D.M. (2006) "Idealized structural unit method and its application to progressive hull girder collapse analysis of ships," *Ships and Offshore Structures*, 1(3), pp. 235–247. Available at: <https://doi.org/10.1533/saos.2006.0129>.
23. Pei, Z. et al. (2015) "Simulation on progressive collapse behaviour of whole ship model under extreme waves using idealized structural unit method," *Marine Structures*, 40, pp. 104–133. Available at: <https://doi.org/10.1016/j.marstruc.2014.11.002>.
24. Wei, P. et al. (2024) "Real-Time Digital Twin of Ship Structure Deformation Field Based on the Inverse Finite Element Method," *Journal of Marine Science and Engineering*, 12(2), p. 257. Available at: <https://doi.org/10.3390/jmse12020257>.

25. Kuznecovs, A. et al. (2020) "Ultimate limit state analysis of a double-hull tanker subjected to biaxial bending in intact and collision-damaged conditions," *Ocean Engineering*, 209, p. 107519. Available at: <https://doi.org/10.1016/j.oceaneng.2020.107519>.
26. Parunov, J., Rudan, S. and Bužančić Primorac, B. (2017) "Residual ultimate strength assessment of double hull oil tanker after collision," *Engineering Structures*, 148, pp. 704–717. Available at: <https://doi.org/10.1016/j.engstruct.2017.07.008>. Author 1, A.B.; Author 2, C.D. Title of the article. *Abbreviated Journal Name* **Year**, *Volume*, page range.

Disclaimer/Publisher's Note: The statements, opinions and data contained in all publications are solely those of the individual author(s) and contributor(s) and not of MDPI and/or the editor(s). MDPI and/or the editor(s) disclaim responsibility for any injury to people or property resulting from any ideas, methods, instructions or products referred to in the content.